

# Light-Harvesting Efficiency Cannot Depend on Optical Coherence in the Absence of Orientational Order

Dominic M. Rouse, Adesh Kushwaha, Stefano Tomasi, Brendon W. Lovett, Erik M. Gauger, and Ivan Kassal\*



Cite This: *J. Phys. Chem. Lett.* 2024, 15, 254–261



Read Online

ACCESS |



Metrics & More

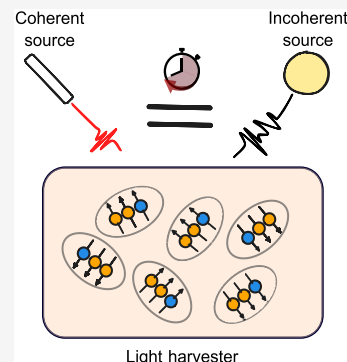


Article Recommendations



Supporting Information

**ABSTRACT:** The coherence of light has been proposed as a quantum-mechanical control for enhancing light-harvesting efficiency. In particular, optical coherence can be manipulated by changing either the polarization state or the spectral phase of the light. Here, we show that, in weak light, light-harvesting efficiency cannot be controlled using any form of optical coherence in molecular light-harvesting systems and, more broadly, those comprising orientationally disordered subunits and operating on longer-than-ultrafast time scales. Under those conditions, optical coherence does not affect the light-harvesting efficiency, meaning that it cannot be used for control. Specifically, polarization-state control is lost in disordered samples or when the molecules reorient on the time scales of light harvesting, and spectral-phase control is lost when the efficiency is time-averaged over a period longer than the optical coherence time. In practice, efficiency is always averaged over long times, meaning that coherent optical control is only possible through polarization and only in systems with orientational order.



Controlling the efficiency of light-harvesting processes using various manifestations of quantum-mechanical coherence has been an active field of research because of the promise of using engineered quantum systems to improve the efficiency of solar energy conversion.<sup>1–16</sup> Some proposals use excitonic coherence, the coherence within the reduced density matrix of the light-harvesting molecules,<sup>17</sup> to enhance the efficiency of excitation capture or retention.<sup>1–6,16,18,19</sup> Other methods instead propose altering the optical coherence, the coherence within the incident light, which can be achieved by manipulating the exciting field.<sup>14,15,20</sup> It is the latter form with which we are concerned here.

Optical coherent control is the manipulation of system observables, such as the light-harvesting efficiency, through changes to the coherence properties of the field.<sup>21</sup> The focus on coherence rules out trivial types of optical control that are based on changing the total power or the spectrum of the light. The variables that affect the coherence but not the spectrum can be seen in the Fourier expansion of a general electric field

$$\mathbf{E}(t) = \frac{1}{\sqrt{2\pi}} \int_{-\infty}^{\infty} d\omega \tilde{\mathbf{E}}(\omega) e^{-i\omega t} \quad (1)$$

where the frequency components are

$$\tilde{\mathbf{E}}(\omega) = e^{i\tilde{\phi}(\omega)} \tilde{E}_0(\omega) \tilde{\mathbf{n}}(\omega) \quad (2)$$

In each frequency component,  $\tilde{\phi}(\omega)$  is the spectral phase while  $\tilde{\mathbf{n}}(\omega)$  indicates the polarization direction.  $\tilde{\mathbf{n}}(\omega)$  is a complex unit vector to allow nonlinear polarizations. To ensure  $\tilde{\phi}(\omega)$  is uniquely defined, we assume the  $x$  component  $\tilde{n}_x(\omega)$  is real. Equation 1 is restricted to a single point in space to avoid

integrals over propagation directions; as we discuss below, this is exact in the electric dipole approximation, which is almost always appropriate for light harvesting.

In general, optical fields are stochastic, meaning that each of the variables  $\tilde{E}_0(\omega)$ ,  $\tilde{\phi}(\omega)$ , and  $\tilde{\mathbf{n}}(\omega)$  is, in each realization of the optical ensemble, a random variable drawn from some distribution. The two strategies for optical coherent control are changes to the distributions from which  $\tilde{\phi}(\omega)$  and  $\tilde{\mathbf{n}}(\omega)$  (but not  $\tilde{E}_0(\omega)$ ) are drawn, because they leave the power spectrum  $\tilde{P}(\omega) = \langle \tilde{\mathbf{E}}(\omega) \cdot \tilde{\mathbf{E}}^*(\omega) \rangle$  unaffected, where  $\langle \cdot \rangle$  is the ensemble average over the stochastic realizations of the field. We call these two approaches spectral-phase control and polarization control.

Both spectral-phase control (through  $\tilde{\phi}(\omega)$ ) and polarization control (through  $\tilde{\mathbf{n}}(\omega)$ ) are possible in certain circumstances. For example, spectral-phase control has been used to modify energy flow in both photosynthetic<sup>22,23</sup> and artificial<sup>24,25</sup> light harvesters and to control the isomerization of retinal.<sup>26</sup> However, all of these examples rely on multiphoton processes achieved in high-intensity laser experiments.<sup>27</sup>

By contrast, practical light harvesting takes place in weak light, where spectral-phase control is also termed one-photon phase control (OPPC).<sup>20,28–37</sup> Weak light means that a

**Received:** October 12, 2023

**Revised:** December 14, 2023

**Accepted:** December 19, 2023

semiclassical first-order perturbation theory in the light–matter interaction is accurate and, therefore, that at most one excitation exists in a molecule at a time. The weak-field approximation is exceptionally accurate for light harvesting because of the low intensity of sunlight; for example, typical chlorophyll excitation rates vary from  $10^{-4} \text{ s}^{-1}$  under overcast conditions to  $10 \text{ s}^{-1}$  in bright sunlight.<sup>38</sup> In closed systems, OPPC is possible for observables that do not commute with the light-independent part of the Hamiltonian.<sup>28,29</sup> Open quantum systems additionally allow for OPPC if the bath interaction couples the population dynamics to the excitonic coherences.<sup>28–30</sup>

Polarization control is also possible in general. A simple example would be a system with all transition dipole moments aligned; light polarized in the direction of the dipoles would be absorbed, while light with perpendicular polarization would not. A less trivial possibility is control through only the degree of coherence between different polarization directions: light-harvesting efficiency in a dimer can be doubled by using polarized light compared to unpolarized light of the same intensity.<sup>14,15</sup> These efficiency gains can be reinforced by stronger coupling to the vibrational baths,<sup>15</sup> conditions relevant for many candidate light-harvesting systems.<sup>4</sup>

However, the control examples given above all assume special circumstances that are unlikely to apply in practical light harvesting. In particular, OPPC proposals rely on the ability to carry out measurements on ultrafast time scales, while the polarization control in refs 14 and 15 assumes a definite relative orientation between the light-harvesting molecules and the incoming light. By contrast, light harvesting almost always occurs over long periods of time in disordered systems; for example, biological chromophores are randomly aligned with respect to sunlight, and their efficiency is averaged over the lifetime of the organism, whether days or years.

Here, we show that in realistic light-harvesting systems neither the efficiency nor any other observable can be controlled by either type of optical coherent control. In realistic cases, the temporal averaging rules out spectral-phase control, while the remaining polarization control is rendered impossible by orientational averaging. These averages are illustrated in Figure 1. We also show what types of coherent control are possible if only one type of averaging takes place, and we show the possibility of optical coherent control, both spectral and polarization, when the averages are partial.

We consider the Hamiltonian

$$H(t) = H_S + H_B + H_{SB} + H_O(t) \quad (3)$$

where  $H_S$  describes a light-harvesting subunit and  $H_B$  describes the environmental bath, which is coupled to the subunit through  $H_{SB}$  and causes dephasing and dissipation among the excited states of the subunit but has no influence on its ground state. The subunit could be, for example, a molecule tumbling in solution or a single unit of a disordered structure, as illustrated in Figure 1b. For light harvesting in weak light, we can describe the light–matter interaction using the semiclassical Hamiltonian

$$H_O(t) = -\sum_{\mu} \mathbf{d}_{\mu} \cdot \mathbf{E}(t) |\mu\rangle \langle G| + \mathbf{E}^*(t) |G\rangle \langle \mu| \quad (4)$$

where  $G$  and  $\mu$  are the ground and excited eigenstates, respectively, of  $H_S$ ,  $\mathbf{d}_{\mu}$  is the transition dipole moment from  $G$  to  $\mu$ , and  $\mathbf{E}(t)$  is the electric field. Assuming that the

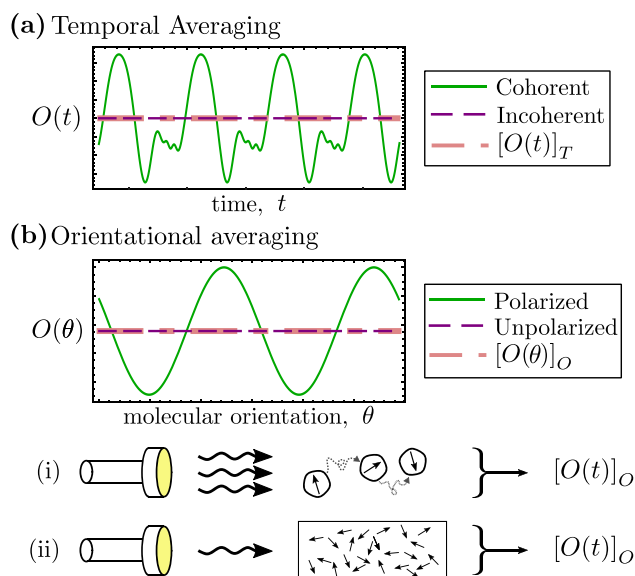


**Figure 1.** Loss of optical coherent control upon averaging. (a) Temporal averaging. The expectation value of an observable is plotted over time for a light field with different spectral coherences.  $[O(t)]_T$  is the temporal average of either the coherent or incoherent processes. (b) Orientational averaging. An observable is plotted as a function of molecular orientation for different polarizations of light.  $[O(\theta)]_O$  is the orientational average of either of the polarization states. Control through the polarization state is lost whether (i) a series of measurements are taken on a reorienting molecule or (ii) a single measurement is taken of a disordered sample.

wavelength of light is larger than the subunit, we can ignore spatial-field dependence; i.e., we make the electric dipole approximation and describe the field using eq 1. Because of the weakness of the field, we can restrict our consideration to the zero- and single-excitation manifolds. Lastly, we have ignored permanent dipole moment interactions in eq 4 because these do not induce transitions to leading order.<sup>39</sup>

Under eq 3, the total density operator of the system and bath evolves as

$$\frac{d}{dt} \rho(t) = \mathcal{L}_{SB} \rho(t) + \sum_{\mu,i} (\mathbf{d}_{\mu} \cdot \mathbf{e}_i) E_i(t) \mathcal{V}_{\mu} \rho(t) + \text{H.c.} \quad (5)$$

where  $\mathcal{L}_{SB} \rho(t) = -i[H_S + H_B + H_{SB}, \rho(t)]$  is the combined system–bath Liouvillian superoperator,  $\mathcal{V}_{\mu} \rho(t) = -i[|\mu\rangle \langle G|, \rho(t)]$  is the optical interaction superoperator, and H.c. denotes the Hermitian conjugate.<sup>20</sup> We have decomposed the field  $\mathbf{E}(t)$  into its Cartesian components  $E_i(t)$  along the directions of unit vectors  $\mathbf{e}_i$  for  $i \in \{x, y, z\}$ .

In section S1 of the Supporting Information, we show that integrating eq 5 to second order in light–matter coupling  $H_O$  and performing the ensemble average yields

$$\langle \rho(t) \rangle = \rho(t_0) + \int_{t_0}^{\infty} d\tau \int_{t_0}^{\infty} d\tau' \sum_{\mu,\nu} R_{\mu\nu}(\tau, \tau') \times \Lambda_{\mu\nu}(t - \tau, \tau - \tau') \rho(t_0) \quad (6)$$

where  $\rho(t_0)$  is the initial density operator, which we take to be a product of the electronic ground state with a thermal bath state. The term that is first-order in  $H_O$  is absent because, for optical fields,  $\langle \mathbf{E}(t) \rangle = 0$ . The optical coherence matrix  $R_{\mu\nu}(\tau,$

$\tau'$ ) and the propagation matrix  $\Lambda_{\mu\nu}(s, s')$  describe two aspects of the light–matter interaction. On the one hand

$$R_{\mu\nu}(\tau, \tau') = \sum_{i,j} \kappa_{\mu\nu ij} G_{ij}(\tau, \tau') \quad (7)$$

describes the coherence properties of the light and its interaction with the system, with

$$\kappa_{\mu\nu ij} = (\mathbf{d}_\mu \cdot \mathbf{e}_i)(\mathbf{d}_\nu \cdot \mathbf{e}_j) \quad (8)$$

being an orientation factor and

$$G_{ij}(\tau, \tau') = \langle E_i(\tau) E_j^*(\tau') \rangle \quad (9)$$

being the two-time correlation function of the field. On the other hand, the propagation matrix

$$\Lambda_{\mu\nu}(s, s') = \mathcal{G}_{\text{SB}}(s) \mathcal{V}_\mu \mathcal{G}_{\text{SB}}(s') \mathcal{V}_\nu \quad (10)$$

describes the full system-bath evolution using Green's function  $\mathcal{G}_{\text{SB}}(t) = \Theta(t) \exp(\mathcal{L}_{\text{SB}}t)$ , with  $\Theta(t)$  being the Heaviside step function. Although eq 6 is perturbative in  $H_0$ , the influence of the bath on the time evolution is incorporated exactly through the propagation matrix.<sup>20</sup>

Because optical coherence is best parametrized in Fourier space, we insert the Fourier transforms of the fields in eq 1 into eq 6, yielding (see section S2 of the Supporting Information)

$$\langle \rho(t) \rangle = \rho(t_0) + \int_{-\infty}^{\infty} d\omega_1 \int_{-\infty}^{\infty} d\omega_2 e^{-i\omega_1 t} \times \sum_{\mu,\nu} \tilde{R}_{\mu\nu}(\omega_1 - \omega_2, \omega_2) \tilde{\Lambda}_{\mu\nu}(\omega_1, \omega_2) \rho(t_0) \quad (11)$$

Functions with tildes and frequency arguments relate to the same functions with temporal arguments by Fourier transforms, using the convention in eq 1. Importantly, the optical coherent control parameters  $\kappa_{\mu\nu ij}$  and  $G_{ij}(\tau, \tau')$  influence the density operator only through the optical coherence matrix  $\tilde{R}_{\mu\nu}(\omega, \omega')$  and not through the propagation matrix  $\tilde{\Lambda}_{\mu\nu}(\omega, \omega')$  (see eqs 7 and 10). Therefore, the central question is how  $\tilde{R}_{\mu\nu}(\omega, \omega')$  is affected by the orientational and temporal averages.

Oriental averaging occurs if the molecules do not have a fixed spatial orientation, which can occur in two ways, as illustrated in Figure 1b. First, the light-harvesting subunit could be tumbling randomly between different light absorption events, as, for example, if the system consists of molecules in solution. Second, a system could be composed of static subunits oriented randomly, such as the molecules in a disordered organic semiconductor. Oriental averaging is the ensemble average over the possible orientations of the tumbling subunit or of the static absorbers in the disordered sample.

Mathematically, orientational averaging involves averaging the orientation of transition dipole moments  $\mathbf{d}_\mu$  within the optical coherence matrix  $\tilde{R}_{\mu\nu}(\omega, \omega')$  over all angles, which affects only the orientation factor  $\kappa_{\mu\nu ij}$ . To distinguish orientational and temporal averages from the optical ensemble average, we denote them with square brackets with subscripts “O” and “T”, respectively. The quantity of interest is  $[\kappa_{\mu\nu ij}]_O$ .

If the subunit is tumbling or disordered in three dimensions,  $\mathbf{d}_\mu$  and  $\mathbf{d}_\nu$  take on all possible values such that  $\mathbf{d}_\mu \cdot \mathbf{d}_\nu$  is fixed. Then, every contribution  $(\mathbf{d}_\mu \cdot \mathbf{e}_i)(\mathbf{d}_\nu \cdot \mathbf{e}_j)$  to the orientational average in  $[\kappa_{\mu\nu ij}]_O$  where  $i \neq j$  is canceled by a contribution of  $(\mathbf{d}_\mu \cdot \mathbf{e}_i)((-\mathbf{d}_\nu) \cdot \mathbf{e}_j)$  from another configuration formed by

rotating the dipoles by 180° around  $\mathbf{e}_i$ . The average of the surviving terms is

$$[\kappa_{\mu\nu ij}]_O = [(\mathbf{d}_\mu \cdot \mathbf{e}_i)(\mathbf{d}_\nu \cdot \mathbf{e}_j)]_O \delta_{ij} \\ = \frac{1}{3} (\mathbf{d}_\mu \cdot \mathbf{d}_\nu) \delta_{ij} \quad (12)$$

where the last equality follows from  $\mathbf{d}_\mu \cdot \mathbf{d}_\nu = \sum_{i \in \{x,y,z\}} (\mathbf{d}_\mu \cdot \mathbf{e}_i)(\mathbf{d}_\nu \cdot \mathbf{e}_i)$ , where each of the three terms on the right-hand side must be equal under orientational averaging because none of the three directions is preferred. Therefore, orientational averaging removes the terms with  $i \neq j$  from the optical coherence matrix.

The quantities of interest for systems operating over long time scales are most commonly time-averaged observables. We now prove that when time-independent observables are averaged over times longer than the coherence time of the incident light, spectral coherence control becomes impossible.

The time-averaged expectation value of a time-independent operator  $O$  is  $[O]_T = [\text{Tr}(O \langle \rho(t) \rangle)]_T = \text{Tr}(O [\langle \rho(t) \rangle]_T)$ , where the time-averaged density operator is

$$[\langle \rho(t) \rangle]_T = \frac{1}{T} \int_{t-T/2}^{t+T/2} dt \langle \rho(t) \rangle \quad (13)$$

with the averaging duration  $T$ , centered at  $t_c$ . The only time-dependent factor in eq 11 is  $e^{-i\omega_1 t}$ , which implies that the integral over time in eq 13 is

$$\frac{1}{T} \int_{t-T/2}^{t+T/2} dt e^{-i\omega_1 t} = e^{-i\omega_1 t_c} \text{sinc}\left(\frac{\omega_1 T}{2}\right) \\ \approx e^{-i\omega_1 t_c} \frac{2\pi}{T} \delta(\omega_1) \quad (14)$$

where the second line holds for  $\omega_1 T \gg 1$ . Because  $\omega_1$  is integrated over in eq 11, the averaging time must be large enough to satisfy  $\omega_1 T \gg 1$  for all values of  $\omega_1$  for which  $|\tilde{G}(\omega_1 - \omega_2, \omega_2)|$  is non-negligible. This implies the requirement that  $T \gg \tau_{\text{coh}}$ , the coherence time of the light, in agreement with earlier results.<sup>31</sup> For sunlight,  $\tau_{\text{coh}} \sim 1$  fs,<sup>40</sup> and for lasers,  $\tau_{\text{coh}}$  can reach 10 s,<sup>41</sup> both of which are much shorter than the days or years over which the performance of light-harvesting systems is typically evaluated.

Inserting eq 14 into eq 11 causes the terms with unequal frequencies to vanish. Therefore, temporal averaging affects the optical coherence matrix as

$$[\tilde{G}_{ij}(\omega, \omega')]_T = \tilde{G}_{ij}(\omega, \omega) \delta(\omega - \omega') \quad (15)$$

We can now assess the effects of orientational and temporal averaging, described by eqs 12 and 15, on the two types of optical coherent control: through the polarization state  $\tilde{\mathbf{n}}(\omega)$  and the spectral phase  $\tilde{\phi}(\omega)$ . These results are summarized in Table 1.

Most importantly, all forms of optical coherent control are impossible under simultaneous orientational and temporal averaging. Substituting the general electric-field expression from eq 1 into eq 7 yields

$$\tilde{R}_{\mu\nu}(\omega, \omega') = \tilde{E}_0(\omega) \tilde{E}_0^*(\omega') e^{i(\tilde{\phi}(\omega) - \tilde{\phi}(\omega'))} \times \sum_{i,j} \kappa_{\mu\nu ij} \tilde{\mathbf{n}}_i(\omega) \tilde{\mathbf{n}}_j^*(\omega') \quad (16)$$

**Table 1.** Effects of Complete Orientational and Temporal Averaging on the Possibility of Optical Coherent Control<sup>a</sup>

average	$\tilde{\phi}(\omega)$ control	$\tilde{n}(\omega)$ control
$[\langle \rho(t) \rangle]_O$	□	■
$[\langle \rho(t) \rangle]_T$	■	□
$[\langle \rho(t) \rangle]_{O,T}$	■	■

<sup>a</sup> ■ denotes that the average always prevents the control. □ denotes that the control remains possible under the average. ■ denotes that the average prevents the control only if the control is independent of frequency.

Using eqs 12 and (15) as well as the normalization  $\sum_i |\tilde{n}_i(\omega)|^2 = 1$ , under simultaneous orientational and temporal averaging eq 16 becomes

$$[\tilde{R}_{\mu\nu}(\omega, \omega')]_{O,T} = \frac{1}{3} |\tilde{E}_0(\omega)|^2 (\mathbf{d}_\mu \cdot \mathbf{d}_\nu) \delta(\omega - \omega') \quad (17)$$

which no longer depends on  $\tilde{n}(\omega)$  or  $\tilde{\phi}(\omega)$ . This scenario, the complete loss of optical coherent control, is by far the most relevant to practical light harvesting. All biological light-harvesting systems and most existing artificial ones involve averages over many randomly oriented subunits and over time scales of days, much longer than the coherence time of any practical light source.

We can also consider the effects of each type of averaging in isolation. Under only temporal averaging

$$[\tilde{R}_{\mu\nu}(\omega, \omega')]_T = |\tilde{E}_0(\omega)|^2 \sum_{i,j} \kappa_{\mu\nu ij} \tilde{n}_i(\omega) \tilde{n}_j^*(\omega) \delta(\omega - \omega') \quad (18)$$

which is independent of  $\tilde{\phi}(\omega)$ , indicating that under temporal averaging, spectral-phase control is impossible. However, temporal averaging does not remove control through the polarization state.

By contrast, under only orientational averaging

$$[\tilde{R}_{\mu\nu}(\omega, \omega')]_O = \frac{1}{3} \tilde{E}_0(\omega) \tilde{E}_0^*(\omega') (\mathbf{d}_\mu \cdot \mathbf{d}_\nu) e^{i(\tilde{\phi}(\omega) - \tilde{\phi}(\omega'))} \times \sum_i \tilde{n}_i(\omega) \tilde{n}_i^*(\omega') \quad (19)$$

Here, both types of control are still possible. However, it is very common for the polarization state to be independent of frequency, in which case orientational averaging removes polarization control, because  $\sum_i \tilde{n}_i(\omega) \tilde{n}_i^*(\omega') = |\tilde{\mathbf{n}}|^2 = 1$  in eq 19.

So far, we have shown that complete averaging causes a loss of coherent control; we now show that both types of optical coherent control are possible if the corresponding averaging is partial. Of course, the partial-averaging results recover the loss of control summarized in Table 1 in the limit of completely averaged orientations and long-time averaging. Throughout this section, we use the light-harvesting efficiency as the observable of interest, although our results hold for any time-independent and isotropic observable of the system.

As a concrete example of our general findings, we demonstrate partial averaging in a model system that is a frequently studied one in the context of light harvesting<sup>2–5,14,15</sup> and is shown in Figure 2. We consider a rigid molecule, approximated as a dimer of two-level sites with excited states, left (|L⟩) and right (|R⟩). The system starts in the ground state (|G⟩) and is illuminated by a pulse. Each site has a transition dipole

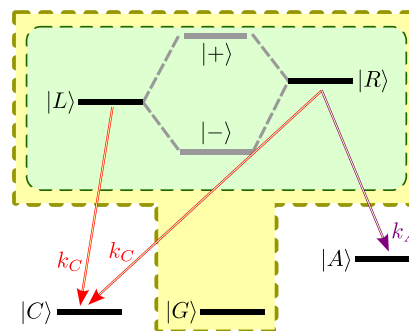


**Figure 2.** Model used for numerical simulations. The yellow area indicates levels affected by  $H_O$  (including the eigenstates of  $H_S$  in gray), and the green area indicates levels affected by  $H_{SB}$ . The arrows show the transitions caused by the Lindblad operators.

moment  $\mathbf{d}_a$  for  $a \in \{L, R\}$ , and the total Hamiltonian is given in eq 3.

The Hamiltonian describing the molecule is

$$H_S = \sum_{a \in \{L, R\}} \varepsilon_a |a\rangle \langle a| + \Omega (|L\rangle \langle R| + |R\rangle \langle L|) \quad (20)$$

where  $\varepsilon_a$  terms are the site energies and excitonic coupling  $\Omega$  is constant due to the rigidity of the molecule. In the eigenbasis,  $H_S = \sum_{\mu \in \{+, -\}} \varepsilon_\mu |\mu\rangle \langle \mu|$ , where the eigenstates  $|\pm\rangle$  have energies  $\varepsilon_\pm = (\varepsilon_L + \varepsilon_R \pm \tilde{\varepsilon})/2$  with  $\tilde{\varepsilon} = ((\varepsilon_R - \varepsilon_L)^2 + 4\Omega^2)^{1/2}$ .

We assume each dipole has an independent but identical bath, typically a vibrational one, described by

$$H_B = \sum_k \sum_{a \in \{L, R\}} \omega_k b_{ka}^\dagger b_{ka} \quad (21)$$

where  $b_{ka}$  annihilates a bath excitation of mode  $k$  on site  $a$ . The system–bath interaction is in the site basis

$$H_{SB} = \sum_k \sum_{a \in \{L, R\}} |a\rangle \langle a| g_k (b_{ka}^\dagger + b_{ka}) \quad (22)$$

and, in the continuum limit, is described by the spectral density  $J(\omega) = \sum_k g_k^2 \delta(\omega - \omega_k)$ , for which we choose a super-ohmic form

$$J(\omega) = \frac{S}{\omega_c^2} \omega^3 e^{-\omega/\omega_c} \quad (23)$$

where  $\omega_c$  is the cutoff frequency and  $S$  is the Huang–Rhys parameter. The super-ohmic form models the broad low-frequency contributions from molecule vibrations.<sup>42</sup> In the numerical analysis, we choose typical values of the parameters in the Hamiltonian, inspired by photosynthetic molecules,<sup>43</sup> but the qualitative conclusions we draw regarding partial averaging are independent of these. We solve the bath evolution using Redfield theory, which is justified for our spectral density choice and weak system–bath interactions.<sup>44</sup>

To calculate the light-harvesting efficiency, we introduce two additional levels that are initially unpopulated: a collector state (|C⟩) and an acceptor state (|A⟩). Once created in the molecule, an excitation will eventually transfer to either the collector or acceptor state via incoherent processes. Transfer to the acceptor models a successful light-harvesting event that contributes to the efficiency, while transfer to the collector models the decay of the excitation, i.e., failed light harvesting. For the sake of simplicity, we add these processes through Lindblad operators

$$L(a, b) = k_b \left( |b\rangle \langle a| \rho |a\rangle \langle b| - \frac{1}{2} \{ |a\rangle \langle a|, \rho \} \right) \quad (24)$$

which models an incoherent transition from  $|a\rangle$  to  $|b\rangle$  at rate  $k_b$ , with  $\{ \cdot, \cdot \}$  being the anticommutator. In our theory, Lindblad operators are included within the evolution terms  $\mathcal{G}_{\text{SB}}(t)$  in eq 10. The specific Lindblad processes we add are shown in Figure 2: decay from  $|L\rangle$  and  $|R\rangle$  to  $|C\rangle$  at rate  $k_C$  and transfer from  $|R\rangle$  to  $|A\rangle$  at rate  $k_A$ . That is, we include  $L(L, C)$ ,  $L(R, C)$ , and  $L(R, A)$ .

The efficiency of the light-harvesting process can be defined in several closely related ways. Here, we consider a quantum efficiency, one proportional to the probability that the excitation makes it to the acceptor state instead of decaying. For the sake of simplicity, we choose

$$\eta(t) = \langle \rho_{AA}(t) \rangle \quad (25)$$

where  $\rho_{aa}(t) = \langle a| \rho(t) |a\rangle$ . This definition is not unique; for example, one could define efficiency as  $\eta'(t) = \langle \rho_{AA}(t) \rangle / (\langle \rho_{AA}(t) \rangle + \langle \rho_{CC}(t) \rangle)$ , which agrees with eq 25 if one excitation is created in the system. However, the definition in eq 25 is easier to measure, more useful in practice, and an observable, unlike  $\eta'(t)$ , which is a ratio of two observables. The latter difference leads to a subtlety in that some polarization control of  $\eta'(t)$  can be lost under partial orientational averages even though observables remain controllable (see section S3 of the Supporting Information).

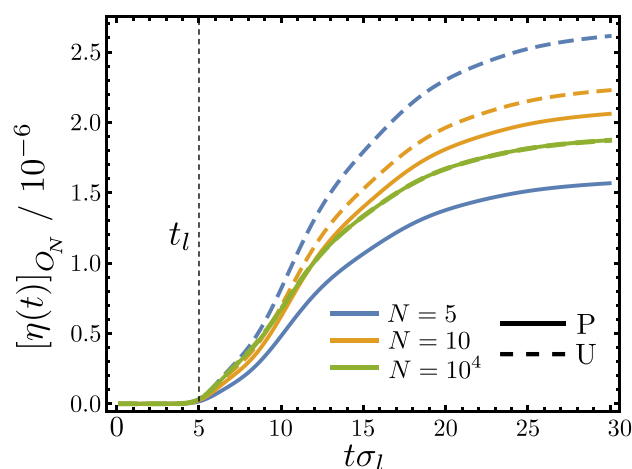
We can now show that the polarization control of the efficiency is possible under partial orientational averaging. For concreteness, we choose a frequency-independent and real  $\tilde{\mathbf{n}}$ , corresponding to linearly polarized light. We do not consider the spectral phase in this example, setting  $\tilde{\phi}(\omega) = 0$ . As the field envelope, we choose a transform-limited Gaussian pulse of frequency width  $\sigma_b$ , central time  $t_b$ , and central frequency  $\omega_l$

$$E(t) = e^{-i\omega_l(t-t_b)} \exp\left(-\frac{1}{2}\sigma_l^2(t-t_b)^2\right) \quad (26)$$

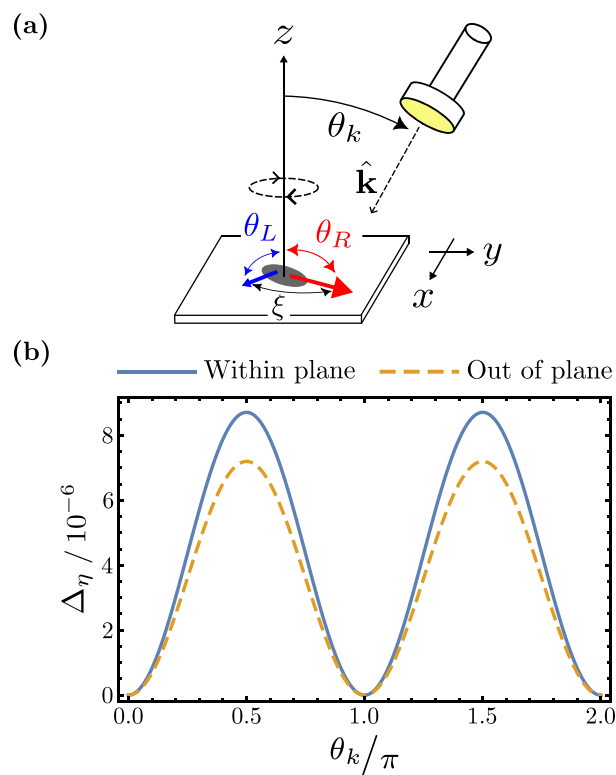
We consider two examples of partial orientational averaging. First, we assume that the molecule is free to tumble in three dimensions, showing that as the number of orientations averaged over becomes large, polarization control is lost. Second, we impose greater orientational restriction by considering a molecule confined to rotations within a plane, a situation that preserves some control through the polarization, even when all of the permitted orientations are averaged.

Figure 3 shows the efficiency for molecules free to tumble in three dimensions. We choose linearly polarized light propagating in the  $z$ -direction, meaning that the polarization is in the  $x$ - $y$  plane,  $\tilde{\mathbf{n}} = \{\tilde{n}_x, (1 - \tilde{n}_x^2)^{1/2}, 0\}$ , determined by the single control parameter  $\tilde{n}_x$ . We consider both  $x$ -polarized light with  $\tilde{n}_x = 1$  and unpolarized light, represented as  $\tilde{n}_x = \cos(\chi)$ , where  $\chi$  is drawn uniformly at random from  $[0, 2\pi]$ . We average the efficiency over  $N$  random orientations of the molecule, which keep the relative angle between the site dipoles fixed at  $\xi = \pi/3$ . Figure 3 shows that for few iterations  $N$ , the efficiencies for the unpolarized and polarized light are different but, in agreement with Table 1, become equal at all times when  $N$  is large. Thus, polarization control in three dimensions is possible under partial orientational averaging.

Figure 4 shows the efficiency when the molecules are restricted to reorient within a plane (the  $x$ - $y$  plane (see Figure 4a)). We again compare  $x$ -polarized and unpolarized light;



**Figure 3.** Polarization control is possible for partial orientational averaging. Efficiency for polarized (P) and unpolarized (U) light in three dimensions after averaging over  $N$  possible dimer orientations. For a small  $N$ , one can control the efficiency by changing the polarization state, but the control is lost at a large  $N$ .  $[\eta(t)]_{O_N}$  is the average over  $N$  iterations, such that  $[\eta(t)]_{O_\infty} = [\eta(t)]_O$ . Parameters used:  $\epsilon_L = 1$  eV,  $\epsilon_R = 1.2$  eV,  $\Omega = 0.05$  eV,  $\sigma_l = \tilde{\epsilon} = \sqrt{(\epsilon_R - \epsilon_L)^2 + 4\Omega^2}$ ,  $S = 0.5$ ,  $\omega_c = 0.5\tilde{\epsilon}$ ,  $k_l = k_r = 0.1\tilde{\epsilon}$ , and  $\xi = \pi/3$ .



**Figure 4.** Polarization control of the efficiency is possible in two dimensions. (a) Schematic showing the relevant angles, and that the molecule can rotate only about the  $z$ -axis. (b) Available polarization control  $\Delta\eta$  (defined in eq 27) over the light-harvesting efficiency as a function of the propagation direction of the light,  $\theta_k$ , averaged over all possible orientations ( $N \rightarrow \infty$ ) in two dimensions. In-plane dipoles have  $\theta_L = \theta_R = \pi/2$ , and out-of-plane dipoles have  $\theta_L = 0.6\pi$  and  $\theta_R = 0.45\pi$ . In both cases,  $\xi = \pi/3$  and  $t_l = 30/\sigma_l$  are fixed. Other parameters are as in Figure 3.

however, because the model is no longer symmetric with respect to the propagation direction of the light, we perform the calculations with the light propagating at each angle  $\theta_i$  in the  $y$ - $z$  plane. For each  $\theta_i$ , we calculate the available optical coherent control averaged over all possible orientations ( $N \rightarrow \infty$ ), defined as

$$\Delta_\eta = |\langle \eta^p(t_f) \rangle_0 - \langle \eta^u(t_f) \rangle_0| \quad (27)$$

where we use the time  $t_f = 30\sigma_l^{-1}$  and  $\eta^p(t)$  and  $\eta^u(t)$  are the efficiencies for the polarized and unpolarized fields, respectively. A larger  $\Delta_\eta$  indicates more available polarization control over the efficiency.

Figure 4b shows that polarization control of the efficiency is impossible only if the light is propagating perpendicular to the plane. Otherwise, the amount of polarization control varies with propagation direction and is maximal when the light is parallel to the plane. This further shows that the limits in Table 1 are guaranteed only for complete (i.e., three-dimensional and across all orientations) averages. Section S3 of the Supporting Information further shows that even though  $\eta(t)$  is controllable, the control of  $\eta'(t)$  can nevertheless be lost.

Finally, we show that spectral-phase control is possible for transient times but is lost under long-time averaging. For this example, we assume that the light is unidirectional and linearly polarized, so that  $\vec{\phi}(\omega)$  is the only remaining control. The effect of the spectral phase is contained within the spectral correlation function

$$\tilde{G}(\omega, \omega') = \tilde{E}_0(\omega)\tilde{E}_0^*(\omega')\langle e^{i\Delta\vec{\phi}(\omega, \omega')} \rangle \quad (28)$$

where  $\Delta\vec{\phi}(\omega, \omega') = \vec{\phi}(\omega) - \vec{\phi}(\omega')$  and  $\tilde{E}_0(\omega)$  is a Gaussian envelope with frequency width  $\sigma_l$ . For the sake of concreteness, we consider a field with

$$\tilde{G}(\omega, \omega') = \tilde{E}_0(\omega)\tilde{E}_0^*(\omega')e^{-\alpha|\omega - \omega'|/2} \quad (29)$$

where  $\alpha$  quantifies the spectral coherence.

For numerical purposes, we construct spectral-phase functions  $\vec{\phi}(\omega)$ , which results in eq 29 on a grid with spacing  $\delta\omega$ . Starting from initial point  $\omega_0$  with phase  $\vec{\phi}(\omega_0)$ , the remaining phases are built using  $\vec{\phi}(\omega_{n\pm 1}) = \vec{\phi}(\omega_n) + \delta\vec{\phi}$ , where phase increments  $\delta\vec{\phi}$  are sampled from a normal distribution of mean 0 and variance  $\alpha\delta\omega$ . Because  $\Delta\vec{\phi}(\omega_{n\pm M}, \omega_n)$  is a sum of  $M$  independent and identically distributed Gaussian random variables, its variance is  $M\alpha\delta\omega = \alpha|\omega_{n\pm M} - \omega_n|$ . Because the characteristic function of a Gaussian random variable  $x$  of mean 0 and variance  $\Sigma^2$  is  $\langle e^{ixt} \rangle = e^{-\Sigma^2 t^2/2}$  we find  $\langle e^{i\Delta\vec{\phi}(\omega, \omega')} \rangle = e^{-\alpha|\omega - \omega'|/2}$ , giving eq 29.

Figure 5 shows the transient light-harvesting efficiency for several values of  $\alpha$ , showing that  $\eta(t)$  depends on, and can be controlled by, the spectral coherence of the light. However, at long times,  $\eta(t)$  is independent of  $\alpha$ . For our choice of electric field, the coherence time  $\tau_{\text{coh}}$  is approximately  $\sigma_l^{-1}$  when  $\alpha = 0$  and increases with  $\alpha$ . As shown in Figure 5, spectral-phase control is possible within the coherence time of the laser but drops off rapidly when  $t - t_l \gg \sigma_l^{-1}$ , in agreement with the discussion following eq 14. Because light-harvesting systems operate on a time scale of days and years, it is clear that for practical purposes spectral-phase control is impossible.

Optical coherence could be used to affect light harvesting in two ways, through the polarization or the spectral phase of the light. Our results show that both of these mechanisms become impossible when the observable of interest, especially the light-

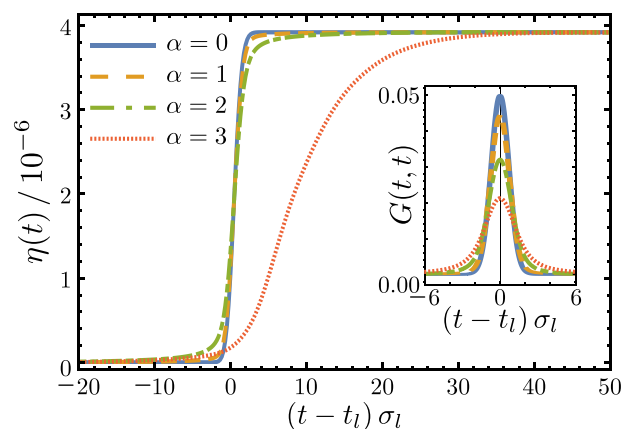


**Figure 5.** Spectral-phase control of light-harvesting efficiency  $\eta(t)$  is possible at short times. The spectral coherence of the light is varied by changing  $\alpha$ , which alters  $\eta(t)$  at short times. However,  $\eta(t)$  is constant at long times, regardless of  $\alpha$ . Parameters are the same as in Figure 3, except that the dipoles are orthogonal and within the  $x$ - $y$  plane, and the pulse is centered at  $t_l = 100\sigma_l$ .  $t_l$  is large so that as little light power as possible is cut off before the numerical integration starts at  $t_0$ . However, because  $t_0 - t_l$  cannot be infinite in numerical calculations, we make tiny scaling corrections to  $G(\omega, \omega')$  to maintain a fixed power (these are purely numerical artifacts). The inset shows the pulse shape intensity, which broadens from a transform-limited Gaussian (spectrally coherent,  $\alpha = 0$ ) to a Lorentzian (spectrally incoherent,  $\alpha \gg 1$ ).

harvesting efficiency, is averaged simultaneously over molecular orientations and time. This situation is by far the most common in natural and artificial light-harvesting systems. However, this does not mean that optical coherence can never affect the light-harvesting efficiency. If the system is subject to only one type of averaging, Table 1 summarizes which types of control are possible. Similarly, if one performs a partial orientational or temporal average (including if molecules are restricted to two dimensions), then some degree of optical coherent control remains possible.

This letter provides a new perspective on the long-standing debate regarding the role that quantum coherence plays in light harvesting. In particular, we have shown that optical coherence is irrelevant to the efficiency of processes in naturally occurring complexes and most practical devices. By contrast, as other works have shown,<sup>1–6,16,18,19</sup> excitonic coherence, in the site or energy basis, offers more promising avenues for optimizing light-harvesting performance.

## ■ ASSOCIATED CONTENT

### Supporting Information

The Supporting Information is available free of charge at <https://pubs.acs.org/doi/10.1021/acs.jpcllett.3c02847>.

Derivation of the time-domain density operator (section S1), Fourier-space density operator (section S2), and controlling the efficiency defined as the ratio of two observables (section S3) (PDF)

## ■ AUTHOR INFORMATION

### Corresponding Author

Ivan Kassal – School of Chemistry and University of Sydney Nano Institute, University of Sydney, Sydney, NSW 2006, Australia; [orcid.org/0000-0002-8376-0819](https://orcid.org/0000-0002-8376-0819); Email: [ivan.kassal@sydney.edu.au](mailto:ivan.kassal@sydney.edu.au)

## Authors

**Dominic M. Rouse** – School of Physics and Astronomy, University of Glasgow, Glasgow G12 8QQ, United Kingdom; Department of Physics and Astronomy, University of Manchester, Manchester M13 9PL, United Kingdom

**Adesh Kushwaha** – School of Chemistry and University of Sydney Nano Institute, University of Sydney, Sydney, NSW 2006, Australia

**Stefano Tomasi** – School of Chemistry and University of Sydney Nano Institute, University of Sydney, Sydney, NSW 2006, Australia

**Brendon W. Lovett** – SUPA, School of Physics and Astronomy, University of St Andrews, St Andrews KY16 9SS, United Kingdom

**Erik M. Gauger** – SUPA, Institute of Photonics and Quantum Sciences, Heriot-Watt University, Edinburgh EH14 4AS, United Kingdom; [orcid.org/0000-0003-1232-9885](https://orcid.org/0000-0003-1232-9885)

Complete contact information is available at:

<https://pubs.acs.org/10.1021/acs.jpcllett.3c02847>

## Notes

The authors declare no competing financial interest.

## ACKNOWLEDGMENTS

D.M.R. was supported by EPSRC Grant EP/T517896. A.K. and I.K. were supported by the Australian Research Council (DP220103584), a Sydney Quantum Academy scholarship, and computational resources from the National Computational Infrastructure (Gadi). E.M.G. acknowledges support from the EPSRC under Grant EP/T007214/1.

## REFERENCES

- (1) Trebbia, J.-B.; Deplano, Q.; Tamarat, P.; Lounis, B. Tailoring the superradiant and subradiant nature of two coherently coupled quantum emitters. *Nat. Commun.* **2022**, *13*, 2962.
- (2) Creatore, C.; Parker, M. A.; Emmott, S.; Chin, A. W. Efficient biologically inspired photocell enhanced by delocalized quantum states. *Phys. Rev. Lett.* **2013**, *111*, 253601.
- (3) Dorfman, K. E.; Voronine, D. V.; Mukamel, S.; Scully, M. O. Photosynthetic reaction center as a quantum heat engine. *Proc. Natl. Acad. Sci. U. S. A.* **2013**, *110*, 2746–2751.
- (4) Fruchtman, A.; Gómez-Bombarelli, R.; Lovett, B. W.; Gauger, E. M. Photocell optimization using dark state protection. *Phys. Rev. Lett.* **2016**, *117*, 203603.
- (5) Rouse, D. M.; Gauger, E.; Lovett, B. W. Optimal power generation using dark states in dimers strongly coupled to their environment. *New J. Phys.* **2019**, *21*, 063025.
- (6) Wertnik, M.; Chin, A.; Nori, F.; Lambert, N. Optimizing cooperative multi-environment dynamics in a dark-state-enhanced photosynthetic heat engine. *J. Chem. Phys.* **2018**, *149*, 084112.
- (7) Gelbwaser-Klimovsky, D.; Aspuru-Guzik, A. On thermodynamic inconsistencies in several photosynthetic and solar cell models and how to fix them. *Chem. Sci.* **2017**, *8*, 1008–1014.
- (8) Fang, J.; Chen, Z.-H.; Su, Y.; Zhu, Z.-F.; Wang, Y.; Xu, R.-X.; Yan, Y. Coherent excitation energy transfer in model photosynthetic reaction center: Effects of non-Markovian quantum environment. *J. Chem. Phys.* **2022**, *157*, 084119.
- (9) Policht, V. R.; Niedringhaus, A.; Willow, R.; Laible, P. D.; Bocian, D. F.; Kirmaier, C.; Holten, D.; Mančal, T.; Ogilvie, J. P. Hidden vibronic and excitonic structure and vibronic coherence transfer in the bacterial reaction center. *Sci. Adv.* **2022**, *8*, eabk0953.
- (10) Romero, E.; Augulis, R.; Novoderezhkin, V. I.; Ferretti, M.; Thieme, J.; Zigmantas, D.; Van Grondelle, R. Quantum coherence in photosynthesis for efficient solar-energy conversion. *Nat. Phys.* **2014**, *10*, 676–682.
- (11) Romero, E.; Novoderezhkin, V. I.; van Grondelle, R. Quantum design of photosynthesis for bio-inspired solar-energy conversion. *Nature* **2017**, *543*, 355–365.
- (12) Cao, J.; et al. Quantum biology revisited. *Sci. Adv.* **2020**, *6*, eaaz4888.
- (13) Tscherbil, T. V.; Brumer, P. Non-equilibrium stationary coherences in photosynthetic energy transfer under weak-field incoherent illumination. *J. Chem. Phys.* **2018**, *148*, 124114.
- (14) Tomasi, S.; Baghbanzadeh, S.; Rahimi-Keshari, S.; Kassal, I. Coherent and controllable enhancement of light-harvesting efficiency. *Phys. Rev. A* **2019**, *100*, 043411.
- (15) Tomasi, S.; Rouse, D. M.; Gauger, E. M.; Lovett, B. W.; Kassal, I. Environmentally improved coherent light harvesting. *J. Phys. Chem. Lett.* **2021**, *12*, 6143–6151.
- (16) Svidzinsky, A. A.; Dorfman, K. E.; Scully, M. O. Enhancing photovoltaic power by Fano-induced coherence. *Phys. Rev. A* **2011**, *84*, 053818.
- (17) Tomasi, S.; Kassal, I. Classification of coherent enhancements of light-harvesting processes. *J. Phys. Chem. Lett.* **2020**, *11*, 2348–2355.
- (18) Davidson, S.; Fruchtman, A.; Pollock, F. A.; Gauger, E. M. The dark side of energy transport along excitonic wires: On-site energy barriers facilitate efficient, vibrationally mediated transport through optically dark subspaces. *J. Chem. Phys.* **2020**, *153*, 134701.
- (19) Davidson, S.; Pollock, F. A.; Gauger, E. Eliminating radiative losses in long-range exciton transport. *PRX Quantum* **2022**, *3*, 020354.
- (20) Mančal, T.; Valkunas, L. Exciton dynamics in photosynthetic complexes: excitation by coherent and incoherent light. *New J. Phys.* **2010**, *12*, 065044.
- (21) Shapiro, M.; Brumer, P. *Quantum Control of Molecular Processes*; John Wiley & Sons, 2012.
- (22) Herek, J. L.; Wohlleben, W.; Cogdell, R. J.; Zeidler, D.; Motzkus, M. Quantum control of energy flow in light harvesting. *Nature* **2002**, *417*, 533–535.
- (23) Wohlleben, W.; Buckup, T.; Herek, J. L.; Motzkus, M. Coherent control for spectroscopy and manipulation of biological dynamics. *ChemPhysChem* **2005**, *6*, 850–857.
- (24) Savolainen, J.; Fanciulli, R.; Dijkhuizen, N.; Moore, A. L.; Hauer, J.; Buckup, T.; Motzkus, M.; Herek, J. L. Controlling the efficiency of an artificial light-harvesting complex. *Proc. Natl. Acad. Sci. U. S. A.* **2008**, *105*, 7641–7646.
- (25) Kuroda, D. G.; Singh, C. P.; Peng, Z.; Kleiman, V. D. Mapping excited-state dynamics by coherent control of a dendrimer's photoemission efficiency. *Science* **2009**, *326*, 263–267.
- (26) Prokhorenko, V. I.; Nagy, A. M.; Waschuk, S. A.; Brown, L. S.; Birge, R. R.; Miller, R. J. D. Coherent control of retinal isomerization in bacteriorhodopsin. *Science* **2006**, *313*, 1257–1261.
- (27) Lavigne, C.; Brumer, P. Interfering resonance as an underlying mechanism in the adaptive feedback control of radiationless transitions: Retinal isomerization. *J. Chem. Phys.* **2017**, *147*, 114107.
- (28) Spanner, M.; Arango, C. A.; Brumer, P. Communication: Conditions for one-photon coherent phase control in isolated and open quantum systems. *J. Chem. Phys.* **2010**, *133*, 151101.
- (29) Pachon, L. A.; Yu, L.; Brumer, P. Coherent one-photon phase control in closed and open quantum systems: A general master equation approach. *Faraday Discuss.* **2013**, *163*, 485–495.
- (30) Pachón, L. A.; Brumer, P. Mechanisms in environmentally assisted one-photon phase control. *J. Chem. Phys.* **2013**, *139*, 164123.
- (31) Lavigne, C.; Brumer, P. Considerations regarding one-photon phase control. *arXiv* **2019**, DOI: 10.48550/arXiv.1910.13878.
- (32) Pachón, L. A.; Brumer, P. Incoherent excitation of thermally equilibrated open quantum systems. *Phys. Rev. A* **2013**, *87*, 022106.
- (33) Arango, C. A.; Brumer, P. Communication: One-photon phase control of cis-trans isomerization in retinal. *J. Chem. Phys.* **2013**, *138*, 02B401.
- (34) Mukamel, S. Coherent-control of linear signals: Frequency-domain analysis. *J. Chem. Phys.* **2013**, *139*, 164113.

(35) Am-Shallem, M.; Kosloff, R. The scaling of weak field phase-only control in Markovian dynamics. *J. Chem. Phys.* **2014**, *141*, 044121.

(36) Shapiro, M.; Brumer, P. Quantum limitations on dynamics and control. *J. Chem. Phys.* **1995**, *103*, 487–488.

(37) Wu, L.-A.; Bharioke, A.; Brumer, P. Quantum conditions on dynamics and control in open systems. *J. Chem. Phys.* **2008**, *129*, 041105.

(38) van Grondelle, R.; Boeker, E. Limits on natural photosynthesis. *J. Phys. Chem. B* **2017**, *121*, 7229–7234.

(39) May, V.; Kühn, O. *Charge and Energy Transfer Dynamics in Molecular Systems*; John Wiley & Sons, 2023.

(40) Ricketti, B. V.; Gauger, E. M.; Fedrizzi, A. The coherence time of sunlight in the context of natural and artificial light-harvesting. *Sci. Rep.* **2022**, *12*, 5438.

(41) Oelker, E.; Hutson, R.; Kennedy, C.; Sonderhouse, L.; Bothwell, T.; Goban, A.; Kedar, D.; Sanner, C.; Robinson, J.; Marti, G.; et al. Demonstration of  $4.8 \times 10^{-17}$  stability at 1 s for two independent optical clocks. *Nat. Photonics* **2019**, *13*, 714–719.

(42) Renger, T.; Marcus, R. A. On the relation of protein dynamics and exciton relaxation in pigment–protein complexes: An estimation of the spectral density and a theory for the calculation of optical spectra. *J. Chem. Phys.* **2002**, *116*, 9997–10019.

(43) Higgins, K. D.; Lovett, B. W.; Gauger, E. Quantum-enhanced capture of photons using optical ratchet states. *J. Phys. Chem. C* **2017**, *121*, 20714–20719.

(44) Breuer, H.-P.; Petruccione, F.; et al. *The Theory of Open Quantum Systems*; Oxford University Press, 2002.